Quantum Quench in an Atomic One-Dimensional Ising Chain

F. Meinert,[1] M. J. Mark,[1] E. Kirilov,[1] K. Lauber,[1] P. Weinmann,[1] A. J. Daley,[2] and H.-C. Nägerl[1]

[1]*Institut für Experimentalphysik und Zentrum für Quantenphysik, Universität Innsbruck, 6020 Innsbruck, Austria*
[2]*Department of Physics and Astronomy, University of Pittsburgh, Pittsburgh, Pennsylvania 15260, USA*

We study nonequilibrium dynamics for an ensemble of tilted one-dimensional atomic Bose-Hubbard chains after a sudden quench to the vicinity of the transition point of the Ising paramagnetic to antiferromagnetic quantum phase transition. The quench results in coherent oscillations for the orientation of effective Ising spins, detected via oscillations in the number of doubly occupied lattice sites. We characterize the quench by varying the system parameters. We report significant modification of the tunneling rate induced by interactions and show clear evidence for collective effects in the oscillatory response.

Ultracold atomic ensembles confined in optical lattice potentials have proven to offer unique access to the study of strongly correlated quantum phases of matter [1,2]. Unprecedented control over system parameters as well as exceptionally good isolation from the environment allow for implementation and quantitative simulation of lattice Hamiltonians [3,4], not only bridging the fields of atomic and condensed matter physics in the study of ground-state phases but also opening fundamentally new opportunities to explore out-of-equilibrium physics in essentially closed quantum systems [5,6]. For example, the rapid time-dependent control available over system parameters makes it possible to observe dynamics arising from a quantum quench, where a parameter such as the lattice depth is changed suddenly in time [7–9]. Recently it was demonstrated that 1D chains of bosonic atoms with a superimposed linear gradient potential exhibit a quantum phase transition to a density-wave-ordered state, in which empty sites alternate with doubly occupied sites ("doublons"). Beginning in a Mott-insulator phase of a Bose-Hubbard (BH) system [10,11], where the on-site interactions dominate over tunneling and the atoms are exponentially localized on individual lattice sites, a gradient potential is added until the potential difference between adjacent sites matches the on-site interaction energy, and atoms can again resonantly tunnel. This was monitored for individual 1D chains with a length of about 10 sites with the quantum gas microscopy technique [12], and effectively maps onto a 1D Ising model [13], making it possible to simulate the transition from 1D paramagnetic (PM) spin chains to antiferromagnetic (AFM) spin chains in the context of ultracold atoms.

In this Letter, we explore the dynamics of a quantum quench for bosonic atoms in such a tilted optical lattice [14–16]. Specifically, we quench the strength of the tilt to be near the phase transition point between PM and AFM regimes, and hence take the system far out of equilibrium, inducing strong oscillations in the number of doublons,

which we detect through molecule formation. We find clear indications for the collective character of the ensuing dynamics.

We consider a 1D atomic ensemble in a tilted optical lattice potential near zero temperature. For sufficiently weak interaction energy, much smaller than the band gap, the system is described by the 1D single-band BH Hamiltonian [10] augmented by a tilt [13,16]

$$\hat{H} = -J\sum_{\langle i,j \rangle} \hat{a}_i^\dagger \hat{a}_j + \sum_i \frac{U}{2}\hat{n}_i(\hat{n}_i - 1) + E\sum_i i\hat{n}_i + \sum_i \varepsilon_i \hat{n}_i. \quad (1)$$

As usual, $\hat{a}_i^\dagger$ ($\hat{a}_i$) are the bosonic creation (annihilation) operators at the ith lattice site, $\hat{n}_i = \hat{a}_i^\dagger \hat{a}_i$ are the number operators, J is the tunnel matrix element, and U is the on-site interaction energy. The linear energy shift from site to site is denoted by E, and ε_i accounts for a weak external confinement. For sufficiently small tilt ($E \ll U$) and sufficiently strong interactions ($U \gg J$) the ground state of the system for one-atom commensurate filling is a Mott insulator with exactly one atom per site. When the tilt is ramped from $E < U$ to $E > U$ across $E \approx U$ at finite J, the system establishes a regular periodic pattern of dipole states, for which one finds double occupancy at every second site with empty sites in between [13,14]; see insets in Fig. 1. The formation of such density-wave ordering is due to an effective nearest-neighbor constraint, which results in correlated tunneling of all particles in the 1D chain. When, in the course of the ramp, the tilt compensates for the interaction energy ($E \approx U$), the particles are allowed to resonantly tunnel onto the neighboring sites, however, only when the neighboring particle has not yet tunneled itself. This system, when $|U - E|, J \ll U, E$, can be mapped onto an effective Ising spin model [12,13], where the two distinct ground states (PM and AFM order, respectively) are connected via a quantum phase transition with the quantum critical point $E_c = U + 1.85J$ [17].
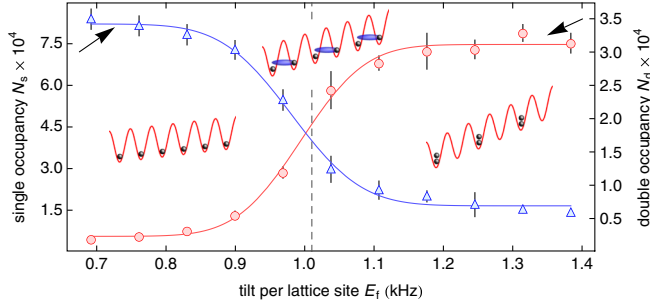
FIG. 1 (color online). Adiabatic tilt through the phase transition point. The number of doublons N_d (circles) as detected through Feshbach molecule formation and the number of singly occupied sites N_s (triangles) are plotted versus the tilt E_f at the end of the adiabatic ramp for $V_z = 10E_R$ and $a_s = 225(5)\,a_0$, giving $U = 0.963(20)$ kHz for $V_{y,z} = 20E_R$. The full ramp takes 40 ms. The solid lines are fits to guide the eye using the error function. The dashed line indicates $E_c = 1.010(20)$ kHz. The insets show a schematic of the Ising phase transition for a 1D Mott-insulator chain from the PM (left) to the AFM (right) ground state [12]. All error bars in this figure and in the following figures denote the one-sigma standard error.

Starting with a Cs Bose-Einstein condensate [18,19] we prepare an ensemble of 1D Bose chains by first creating a 3D Mott insulator in a cubic optical lattice with unity filling (see the Supplemental Material [20]). Initially, the lattice depth V_q is $20E_R$ ($q = x, y, z$), where $E_R = 1.325$ kHz [21] is the photon recoil energy. The residual harmonic confinement along the vertical z direction is $\nu_z = 11.9(0.2)$ Hz. A tilt E of up to 1.7 kHz along z is controlled by a magnetic force $|\nabla B|$. A Feshbach resonance allows us to control U independent of J [22,23].

We first drive the transition adiabatically from the PM to the AFM state. We do this in parallel for an ensemble of about 2000 1D systems ("tubes" or "Ising chains") with an average length of 40 sites (see the Supplemental Material [20]). We start with a pretilt of $E \approx 0.7U$ and then lower V_z to $10E_R$ ($J = 25.4$ Hz [10]) within 10 ms to allow for particle motion along the vertical direction. Effectively, our 3D one-atom-per-site Mott insulator has now turned into an ensemble of 1D tubes with near unity occupation as horizontal tunnel coupling between the tubes can be neglected on the time scale of the experiment. We ramp through the PM-to-AFM transition with a ramp speed of $\dot{E} = 17.3$ Hz/ms up to a final value E_f and project the ensemble of 1D many-body systems onto the number states by quickly ramping V_z up to its initial value and instantly reversing the tilt. We detect double occupancy through Feshbach molecule formation and detection [20,24,25] with an overall doublon detection efficiency of 80(3)%. Figure 1 plots the number of doublons N_d as a function of E_f. The transition from an ensemble of singly occupied sites to an ensemble with predominant double occupation can be seen clearly. The transition point is in very good

agreement with the expectation from the BH model, with $U = 0.963(20)$ kHz and $E_c = 1.010(20)$ kHz. When ramping fully through the transition we create $N_d = 3$ to 4×10^4 doublons, corresponding to ensembles with 79 (2)% double occupancy. We believe that defects in the initial one-atom Mott shell due to finite temperature and the superfluid outer ring are the main limitations to a higher conversion efficiency. We estimate the average length of AFM chains to ≈ 13 lattice sites (see the Supplemental Material [20]). Note that this state with exceptionally high double occupancy is ideal for creating ultracold samples of ground-state molecules [25].

An unambiguous characteristic of a phase transition is its reversibility. Figure 2(a) shows the result when the linear ramp (from 0 to 40 ms) is reversed (from 40 to 80 ms). We find that a large fraction of the doublons, more than 85%, is returned to the one-atom-per-site Mott phase.

Adiabatic driving of the quantum phase transition from the PM into the AFM state is permitted by the finite tunneling rate J between the sites through quantum fluctuations. In Fig. 2(b) we drive the phase transition at various values for the lattice depth V_z in order to highlight the role of tunneling. To assure adiabaticity, we increase the ramp duration for larger V_z. Evidently, a reduced tunnel coupling for larger values of V_z gives rise to a narrowing of the transition. Note that the transition point is shifted to a larger tilt as V_z is increased due to the increase in U. We fit each data set with an error function of the form $\propto$ erf$[(E - E_0)/w]$ and plot the extracted half-width w as a function of V_z in Fig. 2(c). We clearly find the width of the phase transition to scale with the tunnel matrix element. Interestingly, w fits very well to the value $4J$. In Fig. 2(d) we plot the data shown in Fig. 2(b) as a function of $(E_f - U)/J$. The data collapse onto a single curve, confirming the role of J as the natural energy scale [13].

Slow ramping through the critical point allows the system to follow adiabatically the many-body ground state. Nonequilibrium dynamics, however, arises when the initial Mott state is quenched by a rapidly applied tilt to the vicinity of the transition [14,16]. In our experiment we initiate nonequilibrium dynamics by first tilting the lattice and then quickly lowering V_z to $10E_R$. We let the system evolve for a hold time t_h and finally record the number of doublons N_d as before. For the subsequent measurements $U = 1.019(20)$ kHz. Figure 3(a) shows the result for different values of $\delta = E - U$ close to the transition. The ensemble of 1D chains exhibits large amplitude oscillations for N_d. The amplitude is maximal for $\delta \approx 0$ and significantly lower for $|\delta| > 0$. For $\delta \approx 0$, which we call the resonant case, the first maximum is reached at $t_h \approx 3$ ms. The oscillations damp out to an equilibrium value over a time scale of about 30 ms. We fit the data using exponentially damped sinusoids. From these we obtain the frequency f_δ, the peak value of the first oscillation N_d^{max},
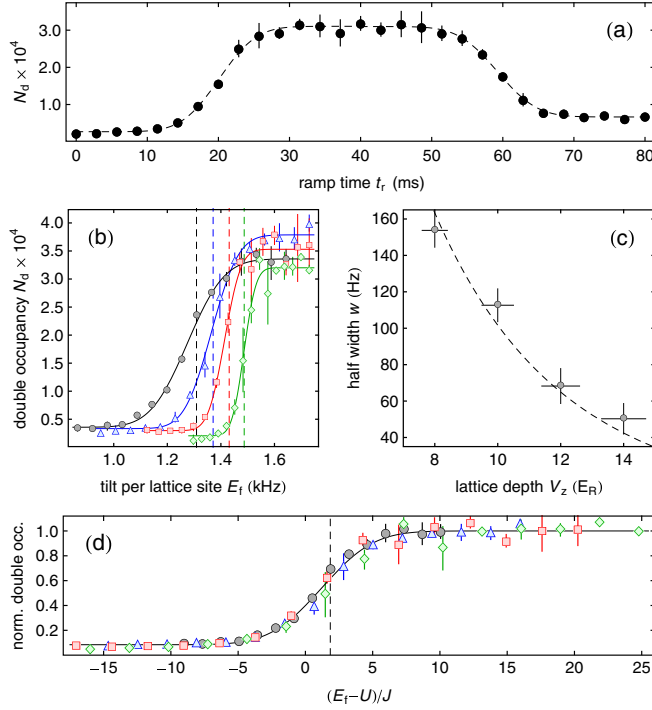
FIG. 2 (color online). (a) Reversibility of the phase transition. The number of doublons N_d is plotted as the system is driven from the PM into the AFM ground state ($t \leq 40$ ms) and back ($t > 40$ ms) for $V_z = 10E_R$. The dashed line is a fit using two concatenated error functions to guide the eye. For this measurement $V_{x,y} = 25E_R$. (b) Phase transition for various values of the lattice depth $V_z = 8$ (circles), 10 (triangles), 12 (squares), and $14E_R$ (diamonds). The ramp rate is $\dot{E} = (17.3, 17.3, 8.6, 5.8)$ Hz/ms for $V_z = (8, 10, 12, 14)E_R$. The solid lines are fits using the error function to determine the half width w. For this measurement $V_{x,y} = 30E_R$. We determine U to (1.233, 1.324, 1.401, 1.467) kHz and E_c to (1.309, 1.371, 1.431, 1.487) kHz for $V_z = (8, 10, 12, 14)E_R$ with typical error of 20 Hz for U and E_c. The positions of E_c are indicated by the dashed lines. (c) Half width w of the phase transition obtained from the fit as a function of V_z. The dashed line shows the calculated $4J$. (d) Same data as in (b) but normalized and plotted as a function of $(E_f - U)/J$. The dashed line indicates the quantum critical point.

and the decay rate γ. Away from resonance, $N_d^{\max}$ is lower; however, f_δ is higher and, interestingly, γ is lower. This can be seen from Figs. 3(b)–3(d), where we plot f_δ, γ, and $N_d^{\max}$ as a function of δ. We fit f_δ by a quadratic function, as will be justified below, and obtain the position of the minimum E_{res}. The data for $N_d^{\max}$ and γ are fitted by Lorentzians. The damping is consistent with collapse of oscillations in coherent dynamics as observed in our simulations of the constrained Ising model (see the Supplemental Material [20]); see also Refs. [13,16]. We find that the positions of the maxima for $N_d^{\max}$ and γ at $E = 1035(2)$ and $E = 1030(3)$ Hz, respectively, agree with the minimum for f_δ at $E_{\text{res}} = 1028(1)$ Hz. Within our error bars [26], all values are compatible with the value
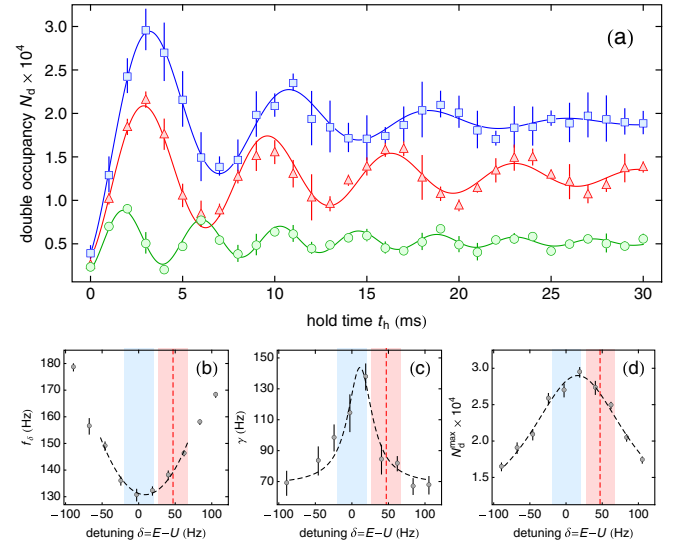

FIG. 3 (color online). Dynamic response for a quench to the resonance point $E \approx U$ with $U = 1.019(20)$ kHz. (a) Number of doublons N_d as a function of hold time t_h for $E = 1.038$ (squares), 0.973 (triangles), and 0.865 kHz (circles). The solid lines are exponentially damped sinusoids fit to the data. (b) Extracted frequency f_δ as a function of $\delta = E - U$. The dashed line is a quadratic fit to the data in the vicinity of the minimum. (c) Extracted damping rate γ as a function of δ. The dashed line is a Lorentzian fit including a finite offset. (d) Extracted number of doublons $N_d^{\max}$ at the first oscillation maximum as a function of δ. The dashed line is a Lorentzian fit. The vertical dashed lines in (b)–(d) give the quantum critical point. The shaded areas (red and blue) indicate the one-sigma statistical experimental error (for $E_c - U$ and $\delta = 0$, respectively). For all measurements $V_z = 10E_R$, $V_{x,y} = 20E_R$, and $a_s = 238(5)\, a_0$.

for U. We note that $N_d^{\max}$ is only about 5% lower than the value for N_d we obtained from the adiabatic sweep as shown in Fig. 1.

The quadratic fit to the data for f_δ is justified, in the simplest approximation, by a two-state Rabi model for the case of a single double-well potential [14]. At the point $E \approx U$, the two Fock states $|11\rangle$ and $|20\rangle$, describing one atom in each site and two atoms in the left site, respectively, are resonantly coupled by J, leading to Rabi oscillations between the two states with frequency $\sqrt{2}J$, where the factor $\sqrt{2}$ ensues from bosonic enhancement. The probability to find the system in the dipole state $|20\rangle$ thus oscillates in the case of finite detuning from resonance with the generalized Rabi frequency $f_\delta = \sqrt{8J^2 + \delta^2}$ [14], which is quadratic for sufficiently small δ.

Before we continue this discussion we make use of our capability to tune U by means of a Feshbach resonance. We repeat the measurements shown in Fig. 3 for different values of a_s to which we tune after producing the 3D one-atom Mott-insulator state and before initializing the quench. We determine the resonance position E_{res} and the
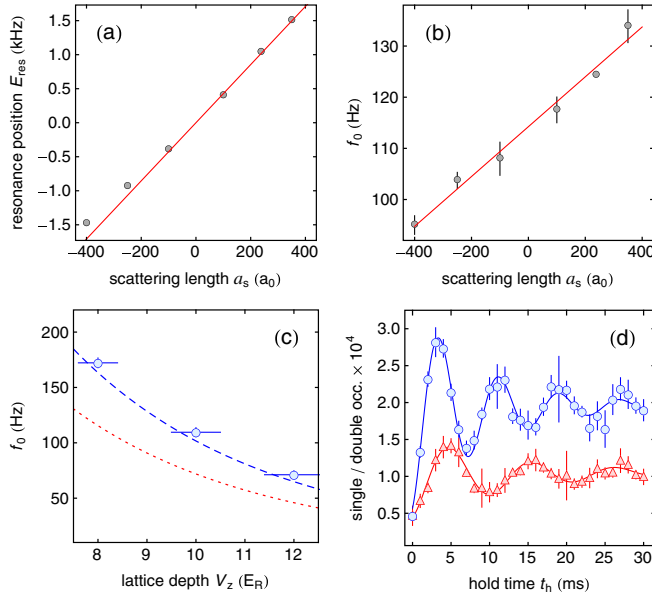
FIG. 4 (color online). Dependence of the resonance position $E_{\rm res}$ (a) and of the on-resonance oscillation frequency f_0 (b) on a_s as deduced from the dynamical response of the system. The solid line in (a) is the linear prediction of the BH model. In (b) the solid line is a linear fit to the data. For these measurements, $V_z = 10E_R$ and $V_{x,y} = 20E_R$. (c) On-resonance oscillation frequency f_0, interpolated to $a_s = 0$, as a function of V_z (circles). The dashed and dotted lines show the expected result for an Ising chain of three sites and the double well in the noninteracting limit, respectively. (d) On-resonance quench dynamics for the number of doublons in the 1D Ising chain (circles) and the number of singly occupied sites in nearly isolated double wells (triangles) for $U = 1.060(20)$ kHz.

on-resonance oscillation frequency $f_0 = f_{\delta=0}$. The result is shown in Figs. 4(a) and 4(b). For repulsive interactions we find good agreement for $E_{\rm res}$ with U calculated from lowest-band Wannier functions [10]. For attractive interactions there is a significant shift to lower absolute values of $E_{\rm res}$ as corrections taking into account higher bands and the properly regularized pseudopotential would have to be included [23]. We attribute the considerable dependence of the data for f_0 on a_s to an effectively altered tunnel barrier as U and hence $E_{\rm res}$ are changed [27,28].

We now quantitatively compare our findings for f_0 with the result from the simplified double-well system. First, to remove the effects of the modified tunneling rate due to the tilt and interactions, we interpolate our data to find f_0 for $a_s = 0$ with the linear fit as shown in Fig. 4(b). The resulting values are shown in Fig. 4(c) for data sets taken at three different values of V_z and are compared to the prediction for the double well on resonance, $f_0 = 2\sqrt{2}J$ (dotted line). Evidently, the tunneling in the 1D chains is significantly faster when compared to the double-well system. This arises due to the nearest-neighbor constraint present in the 1D chains, which prohibits having two adjacent dipoles and which leads to an increase of the

oscillation frequency even for three sites by a further factor of $\sqrt{2}$, to $4J$ (dashed line) [14]. Through numerical simulations with up to 60 lattice sites we have verified that the oscillation frequency shows only a slight further increase for longer chains beyond 3 sites (see the Supplemental Material [20]). The weak harmonic trapping potential causes an additional small increase of the computed oscillation frequency. However, both effects are presently within our experimental uncertainty.

Finally, we compare the on-resonance oscillatory dynamics of the ensemble of 1D Ising chains with that of an ensemble of nearly isolated effective double-well systems to check the role of the constraint. The double wells are engineered by highly nonadiabatic loading of the 3D lattice, thereby creating a comparatively dilute sample of doublons. We clean out the singly occupied lattice sites by temporarily hiding the doublons in a molecular state and removing singular atoms by resonant light. We subsequently initiate the quench dynamics as before and detect the number of singly occupied sites (see the Supplemental Material [20]) as a function of t_h as shown in Fig. 4(d). The oscillation frequencies in the two systems, determined to $f_0 = 128(2)$ Hz and $f_0 = 93(2)$ Hz, respectively, differ by a factor 1.38(3), in good agreement with the collective effect discussed above.

In conclusion, we have investigated quench dynamics by tuning a tilt suddenly onto the transition from PM to AFM Ising order in a large ensemble of 1D atomic Mott-insulator chains. We observe significant shifts of the tunneling parameter arising from interactions, and collective effects in the oscillations arising from the effective constraint in the model. This study of quench dynamics opens the opportunity to explore many aspects of the dynamics in these systems that up to now were only addressed theoretically. This includes scaling relations for smaller quenches across the phase transition [15,29,30], as well as possibly quenches at other resonance points (e.g., near $E = U/2$).

[1] O. Morsch and M. Oberthaler, Rev. Mod. Phys. **78**, 179 (2006).
[2] I. Bloch, J. Dalibard, and W. Zwerger, Rev. Mod. Phys. **80**, 885 (2008).
[3] M. Lewenstein, A. Sanpera, V. Ahufinger, B. Damski, A. Sen De, and U. Sen, Adv. Phys. **56**, 243 (2007).
[4] S. Sachdev, Nat. Phys. **4**, 173 (2008).
[5] A. Polkovnikov, K. Sengupta, A. Silva, and M. Vengalattore, Rev. Mod. Phys. **83**, 863 (2011).
[6] I. Bloch, J. Dalibard, and S. Nascimbne, Nat. Phys. **8**, 267 (2012).

[7] M. Cheneau, P. Barmettler, D. Poletti, M. Endres, P. Schauß, T. Fukuhara, C. Gross, I. Bloch, C. Kollath, and S. Kuhr, Nature (London) **481**, 484 (2012).

[8] S. Trotzky, Y-A. Chen, A. Flesch, I. P. McCulloch, U. Schollwöck, J. Eisert, and I. Bloch, Nat. Phys. **8**, 325 (2012).

[9] S. Will, T. Best, U. Schneider, L. Hackermüller, D. S. Lühmann, and I. Bloch, Nature (London) **465**, 197 (2010).

[10] D. Jaksch, C. Bruder, J. I. Cirac, C. W. Gardiner, and P. Zoller, Phys. Rev. Lett. **81**, 3108 (1998).

[11] M. Greiner, O. Mandel, T. Esslinger, T. W. Hänsch, and I. Bloch, Nature (London) **415**, 39 (2002).

[12] J. Simon, W. S. Bakr, R. Ma, M. E. Tai, P. M. Preiss, and M. Greiner, Nature (London) **472**, 307 (2011).

[13] S. Sachdev, K. Sengupta, and S. M. Girvin, Phys. Rev. B **66**, 075128 (2002).

[14] C. P. Rubbo, S. R. Manmana, B. M. Peden, M. J. Holland, and A. M. Rey, Phys. Rev. A **84**, 033638 (2011).

[15] M. Kolodrubetz, D. Pekker, B. K. Clark, and K. Sengupta, Phys. Rev. B **85**, 100505 (2012).

[16] A. R. Kolovsky, Phys. Rev. A **70**, 015604 (2004).

[17] S. Sachdev, *Quantum Phase Transitions* (Cambridge University Press, Cambridge, England, 1999).

[18] T. Weber, J. Herbig, M. Mark, H.-C. Nägerl, and R. Grimm, Science **299**, 232 (2002).

[19] T. Kraemer, J. Herbig, M. Mark, T. Weber, C. Chin, H.-C. Nägerl, and R. Grimm, Appl. Phys. B **79**, 1013 (2004).

[20] See Supplemental Material at http://link.aps.org/supplemental/10.1103/PhysRevLett.111.053003 for details on the preparation of the single-atom-per-site Mott insulator, calibration of the tilt E and onsite interaction energy U, estimation of the average lengths of Mott chains, detection methods of single and double occupancy, and numerical simulations of the quench dynamics.

[21] We give all energies in frequency units.

[22] M. J. Mark, E. Haller, K. Lauber, J. G. Danzl, A. J. Daley, and H.-C. Nägerl, Phys. Rev. Lett. **107**, 175301 (2011).

[23] M. J. Mark, E. Haller, K. Lauber, J. G. Danzl, A. Janisch, H. P. Büchler, A. J. Daley, and H.-C. Nägerl, Phys. Rev. Lett. **108**, 215302 (2012).

[24] K. Winkler, G. Thalhammer, F. Lang, R. Grimm, J. Hecker Denschlag, A. J. Daley, A. Kantian, H. P. Büchler, and P. Zoller, Nature (London) **441**, 853 (2006).

[25] J. G. Danzl, M. J. Mark, E. Haller, M. Gustavsson, R. Hart, J. Aldegunde, J. M. Hutson, and H.-C. Nägerl, Nat. Phys. **6**, 265 (2010).

[26] We note that the day-to-day variation of the positions of the extrema for N_d^{max}, γ, and f_δ is about 10 Hz and hence considerably larger than the statistical error from the fits.

[27] U. Bissbort, F. Deuretzbacher, and W. Hofstetter, Phys. Rev. A **86**, 023617 (2012).

[28] D. S. Lühmann, O. Jürgensen, and K. Sengstock, New J. Phys. **14**, 033021 (2012).

[29] M. Kolodrubetz, B. K. Clark, and D. A. Huse, Phys. Rev. Lett. **109**, 015701 (2012).

[30] C. De Grandi, V. Gritsev, and A. Polkovnikov, Phys. Rev. B **81**, 012303 (2010).